

A Search for Sodium Absorption from Comets Around HD209458

Caylin Mendelowitz¹, Jian Ge¹, Avi M. Mandell¹, and Aigen Li²

ABSTRACT

We monitored the planet-bearing solar-type star HD209458 for sodium absorption in the region of the stellar NaI D1 line that would be indicative of cometary activity in the system. We observed the star using the HET HRS with high S/N and high spectral resolution for 6 nights over the course of two years, from July 2001 to July 2003. From modelling we determine a 20% likelihood of a detection, based on a predicted number of comets similar to that of the solar system. We find that our analytical method is able to recover a signal and our S/N is sufficient to detect this feature in the spectral regions on either side of the core of the D1 line, where it is most likely to appear. No significant absorption was detected for any of the nights based on a 3σ detection limit. We derive upper limits on the column density of sodium of $\lesssim 6 \times 10^9 \text{ cm}^{-2}$ for a signal in the region around the line core and $\lesssim 2 \times 10^{10} \text{ cm}^{-2}$ for a signal in the core of the photospheric D1 line. These numbers are consistent with the sodium released in a single periodic comet in our own system, though higher S/N may be necessary to uncover a signal in the core of the D1 line. Implications for cometary activity in the HD209458 system are discussed.

Subject headings: planetary systems:formation and detection- stars:individual(HD209458)
- techniques:spectroscopic - comets:general

1. Introduction

The Falling Evaporating Bodies (FEB) scenario (Lagrange *et al.* 1992) was introduced as an explanation for time variable circumstellar absorption features observed in the spectral lines of the A-type star β Pictoris (Lagrange *et al.* 1986; Beust *et al.* 2000). Similar features

¹Pennsylvania State University, Department of Astronomy & Astrophysics, University Park, PA 16802, USA Email: caylinm@astro.psu.edu, jian@astro.psu.edu, mandell@astro.psu.edu

²Theoretical Astrophysics Program, Steward Observatory, and Lunar & Planetary Laboratory, University of Arizona, Tucson, AZ 85721, USA Email: agli@lpl.arizona.edu

have also been observed in other early-type main sequence stars and some Herbig Ae/Be stars, which are considered β Pictoris precursors (Welsh *et al.* 1998; Grady *et al.* 1997; Grinin *et al.* 1996). According to the FEB hypothesis, solid bodies with sizes typical of solar system comets, are evaporated within the vicinity of the star producing absorption lines when observed along the line of sight (Ferlet *et al.* 1987; Lagrange *et al.* 1988). The high frequency of infalling comets is a phenomenon invoked in models of the early solar system and corresponds to the clearing out stage in a system’s formation (Welsh *et al.* 1998; Beust *et al.* 1998). The mechanism behind the infall of these bodies is thought to be from the gravitational perturbation by at least one planet (Beust *et al.* 2000). Monitoring known planet-bearing solar analogs for comet activity would then give insight into the evolution of an exosolar system and such a wide study would investigate how comet populations evolve in time and with stellar mass. Also, searches for comet disks and clouds orbiting other stars offers a new method for inferring the presence of planetary systems (Stern 1993).

Sungrazing comets and periodic comets are quite frequent in our own system. Since the first light of the SOLar and Heliospheric Observatory (SOHO) Large Angle and Spectrometric COronograph (LASCO) on 1995 December 30 over 600 new sungrazing comets have been discovered ($\sim 60/\text{year}$) (SOHO Sungrazer website). Also, the number of catalogued periodic comets totals ~ 900 with half having perihelia ≤ 1 AU (Biswas 2000). Comets evaporate a significant amount of material as they approach perihelion in the form of a coma and tails. For example, Halley’s comet loses ~ 0.001 of its mass every perihelion passage ($\sim 10^{11}\text{kg}$) (Zeilik & Gregory 1998). Hale-Bopp is a richer dust factory: in its 1997 apparition, it lost a total dust mass of $\sim 3 \times 10^{13}$ kg (Jewitt & Matthews 1999). The absorption features expected for many species known to be present in comets are quite weak due to the small column densities. Cremonese *et al.* (1997) discovered the sodium tail in comet C/1995 O1 Hale-Bopp, which is a third type of cometary tail consisting of neutral atoms. Sodium has also been observed in the tail of some other bright comets and in the comae of comets that were located at around 1 AU from the Sun (e.g., comet 1P/Halley) (Wanatabe *et al.* 2003). Sodium is a good candidate for extra-solar detection because it is detectable even when the column density is low (Cremonese *et al.* 1997), and sodium has already been detected in absorption from gas in the β Pictoris disk (Hobbs *et al.* 1985), in variable absorption in some Herbig Ae/Be stars (Sorelli *et al.* 1996), and in the atmosphere of the exosolar planet HD 209458b (Charbonneau *et al.* 2002).

HD209458 is a solar-type star with a close-in Jovian-type planet. It is oriented edge-on to our line of sight making it an ideal candidate for absorption spectroscopy and the detection of orbiting bodies. This has initiated several new exoplanet discoveries. It is the first exosolar system for which repeated transits across the stellar disk have been observed (Charbonneau *et al.* 2000). This allowed Charbonneau *et al.* (2002) to make the first observation of an exosolar

planet atmosphere through the detection of neutral sodium absorption. More recently, Vidal-Madjar *et al.* (2003) detected atomic hydrogen which is associated with the upper atmosphere of the planet. Here we observe HD209458 for neutral sodium absorption from a comet crossing the line of sight. We present spectra of HD209458 in the vicinity of the Na D1 line (5895.9243 Å). In §2 we present the data and describe the data reduction technique. We analyze the data and remove the photospheric contribution of sodium. In §3 we use our simulation of a cometary sodium absorption feature to examine its position in relation to the photospheric sodium line and its shape based on expected values of the column density, in order to define a search region. A synthetic spectrum is analyzed to check the reliability of our method. In §4 we examine the residuals, discuss the results and derive upper limits for the column density of sodium on each night. We use modelling to determine the likelihood of detecting a comet and conclude with possible explanations for the non-detection and a discussion of comet activity in the system.

2. Observations & Analysis

Observations of HD209458 were made with the High Resolution Spectrograph (HRS) at the 9.2 meter Hobby-Eberly Telescope (HET) (Tull 1998). The HRS is a fiber-coupled echelle spectrograph, using an R-4 echelle mosaic with cross-dispersing gratings. The camera images onto a mosaic of two 2K x 4K CCDs with 15 μm pixels and a gap between them that spans ~ 72 pixels. The spectrograph was used in high-dispersion mode, with an average resolving power of $R = \lambda/\Delta\lambda \sim 115,000$ measured from thorium lines, corresponding to a resolution element of ~ 0.049 Å in the region of interest. The spectral coverage for the cross disperser setting used is between 4076 Å and 7838 Å. Observation dates and parameters are listed in Table 1. The star HD12235 was also observed to serve as a reference system. We observed for two nights on 2002 August 28 and 31, using the same instrumental settings as HD209458. Stellar parameters are listed in Table 2.

Images typically had an integration time of 5 to 25 minutes depending on brightness, and a total integration time between 1 and 2 hours. A Thorium-Argon lamp was observed before and after each sequence of exposures. Due to sodium emission lines in the flatfield illumination lamp, it was necessary to use extremely high S/N observations of rapidly rotating B and A stars as flat fields. These calibration stars were observed as near in time to the program stars as possible. The data were reduced using the publically available IRAF software package. Continuum normalization was performed by selecting continuum regions in each image without obvious absorption lines or bad pixels and fitting a higher order polynomial to these sections. Images were then combined with appropriate rejection algorithms. Wave-

length calibration of the spectra was obtained using the Thorium-Argon lamp comparison spectra for each data set. The 2002 December 9 data was missing a calibration star so the lamp was used for flatfielding, with the sodium emission lines removed using a polynomial fit to obtain a featureless spectrum. The S/N per pixel in the continuum for each image is listed in Table 3. Figure 1 shows the reduced spectra for HD209458 for each of the 6 nights. The spectra have been shifted to the rest frame of HD209458.

The D1 line was used for analysis since the D2 line is heavily contaminated by telluric lines (Ge 1998). The broad photospheric sodium line was removed using a polynomial fit (see Figure 1), including multiple rejection iterations and the normalized spectrum was searched for possible narrow absorption features up to 0.7 \AA from the photospheric line center. Several absorption features above 3σ were attributed to telluric features that were removed imperfectly due to changes in observing conditions between exposures of HD209458 and the calibration star. This is the case for the 2002 October 10 spectrum where there is a significant absorption feature around 5896.5 \AA ; the feature is also present in the calibration star used for flatfielding. For 2001 July 7 observing conditions were deteriorated by the fourth exposure, which is the cause of the absorption feature near 5895.86 \AA . No absorption features greater than 3σ due to cometary activity were identified.

3. Modelling

Simulations were run to produce estimates of the position and shape of a sodium absorption feature due to solar-like comets in the HD209458 system. Constraints on spatial and chemical characteristics of cometary bodies were taken from observations of short and long period comets in our own system, mainly the comets Halley and Hale-Bopp (Krishna Swamy 1997; Zeilik & Gregory 1998; Cremonese *et al.* 1997). Although sungrazing comets also display tail and coma features, they are much smaller than periodic comets, only a few meters to a few tens of meters (Iseli *et al.* 2002) (whereas periodic comets are a few kilometers to hundreds of kilometers), and therefore will not release a significant amount of dust. The position of the feature will depend on the velocity of the comet when detected; as a comet moves within $\sim 3 \text{ AU}$ the cometary nucleus begins to display coma formation followed by the extension of gas and ion tails. Full display of the comet tail occurs between 1.0 and 1.5 AU, (Biswas 2000) with sodium extending beyond 10^5 km from the nucleus (Oppenheimer 1980). In Hale-Bopp the length of the sodium tail was measured to be $3 \times 10^7 \text{ km}$ (Cremonese 1997). In order to obtain the maximum column density along the line of sight, a theoretical comet velocity was calculated specifically for an orientation aligned with the sodium tail, which points roughly anti-sunward. Since the radius and luminosity of HD209458 are larger than

for the Sun, the orbital distance for detecting the sodium tail was set to within 3 AU of the star.

The wavelength shift due to the orbital motion of the comet with respect to the parent star is described by the radial velocity of the comet:

$$v_r = (2a/P)(e \sin \theta)(1 - e^2)^{-1/2} \quad (1)$$

where e is the eccentricity, a is the semi-major axis, P is the period and θ is measured so that $\theta=0$ is at perihelion. The distance from the star is given by:

$$r = \frac{a(1 - e^2)}{e \cos \theta + 1} \quad (2)$$

The range of velocity shifts for a spectral feature have been calculated using the parameters of the short-period (SP) comet Halley ($e=0.967$, $a=18$ AU, $P=76$ years, perihelion distance $q=0.587$ AU) and the long-period (LP) comet Hale-Bopp ($e=0.9951$, $a=187$ AU, $P=2550$ years, $q=0.914$ AU). Figure 2 shows the wavelength and corresponding doppler shift for both types of comet. The velocity and thus the wavelength shift for Halley peaks at 1.17 AU, with a maximum shift of 0.53 \AA from the photospheric line center. For Hale-Bopp the maximum velocity is reached at 1.83 AU, which results in a maximum wavelength shift of 0.43 \AA . The majority of the orbit, from $\sim 1\text{-}3$ AU, for both types of comet will produce a wavelength shift of $\sim 0.4 \text{ \AA}$. Since the D1 line is $\sim 0.6 \text{ \AA}$ wide, a feature will most likely be in the wing or continuum region. We also take into consideration the periodic comets with perihelia less than those of Halley and Hale-Bopp (~ 220 comets (Biswas 2000)), which would produce a greater wavelength shift. Our search for Na absorption will be $\pm 0.7 \text{ \AA}$ around the stellar Na D1 line.

The depth and shape of the feature depends on the column density and temperature of the absorbing material. A model of the signal was created using a Voigt absorption profile, which was then convolved with the instrumental spectral resolution. Figure 3 shows model absorption lines based on the core and continuum upper limits derived for our best S/N data, 2002 December 9, in §4.1. Estimates of the column density of sodium from evaporating comets in other systems are on the order of 10^{10} cm^{-2} from HR10 (FEB) (Welsh *et al.* 1998) and from β Pictoris (disk) (Hobbs *et al.* 1985). The thermal broadening can be calculated by assuming a gas temperature for the comet coma and tail. The estimated temperature for the sodium tail of a comet, from solar system observations, is 150K (Krishna Swamy 1997), and atomic parameters for the sodium D1 line were taken from Morton (1991). The inherent Doppler width at 150K corresponds to only 0.03 \AA , and therefore a single radial velocity absorption component would be spectrally unresolved, with the instrumental FWHM of 0.049 \AA of the HRS. The equivalent width of a sodium absorption line with a column density of 10^{10} cm^{-2} is $\sim 1 \text{ m\AA}$.

3.1. Synthetic Detection: Check on the Analysis

As a check of our analytical method we input our synthetic absorption features into the observed spectrum and recover the absorption through fitting the broad stellar sodium D1 line profile. We use the data from 2002 November 23 since telluric features have been successfully removed and the S/N is the highest (They were not removed in 2002 December 9). Since the detection limit is lower in the continuum than in the core of the line, we place the feature in the continuum (S/N=237) with a column density of $6.4 \times 10^9 \text{ cm}^{-2}$ and in the core (S/N=88) with a column density of $1.7 \times 10^{10} \text{ cm}^{-2}$ derived in §4.2 as the 3σ upper limits for this date. We also place a feature in the wing of the line with a column density of $9.3 \times 10^9 \text{ cm}^{-2}$ based on a calculated S/N of 162. The feature was added at the stage just before the removal of the photospheric D1 line. Our method of polynomial fitting was able to recover the features at the core, wing and also continuum region. The residuals and recovered absorption features are shown in Figure 4. The equivalent width of the recovered features are 1.6 ± 0.6 , 1.0 ± 0.3 , and $0.62 \pm 0.2 \text{ m\AA}$, for the core, wing, and continuum respectively. These are all consistent with the input values of 1.7, 0.9, and 0.6 m\AA , for the core, wing, and continuum respectively. This demonstrates proof that the stellar D1 line profile fitting technique can recover narrow sodium features from comet events.

4. Results and Discussion

4.1. Upper Limits on Sodium Column Density by Comets

The residual after the photospheric sodium line is removed are shown in Figure 5. No signal was detected in any of the spectra, but upper limits were determined based on a 3σ detection limit. The 1σ upper limit to the equivalent width for the undetected feature was determined by:

$$W_\lambda = \int \frac{F_c - F_\lambda}{F_c} d\lambda \approx \Delta\lambda \times \sigma \quad (3)$$

where F_c is the normalized flux in the continuum, F_λ is the normalized absorption line, $\Delta\lambda$ is the spectral resolution element 0.049 \AA , and σ is:

$$\sigma(\lambda) = \frac{1}{F_\lambda I_c(\lambda)} \{F_\lambda I_c(\lambda) + p\varepsilon^2\}^{1/2} \approx \frac{1}{S/N} \quad (4)$$

$I_c(\lambda) = N_c \times \text{gain}$, where N_c is the number of counts in the continuum and $\text{gain} = 0.6320 \text{ e}^- \text{ ADU}^{-1}$, ε is the readnoise 2.70 e^- , and p is the pixel number in the cross-slit direction used for sampling a spectrum. It is appropriate to assume that the absorption line is in the linear portion of the curve of growth, where the column density is proportional to the equivalent

width. The integrated number of sodium atoms per square centimeter in the line of sight is then given by:

$$N = \frac{mc^2}{\pi e^2 f} \int_0^\infty \frac{F_c(v) - F(v)}{F_c(v)} dv = 1.130 \times 10^{20} \frac{W_\lambda}{f \lambda^2} cm^{-2}, \quad (5)$$

where f is the oscillator strength ($f=0.318$ for 5895.9243 (Morton 1991), and W_λ and λ are in units of Angstroms. The upper limits for each date are given in Table 3. In the continuum region, the column density for each night ranges from $\sim 6 \times 10^9 - 2 \times 10^{10} \text{ cm}^{-2}$, whereas in the region of the D1 line core upper limits range from $\sim 2 \times 10^{10} - 7 \times 10^{10} \text{ cm}^{-2}$. This appears to be consistent with the solar comet sodium column density (e.g., sodium absorption from an occultation of the solar system comet Giacobini-Zinner resulted in upper limits of $N(\text{NaI}) < 2 \times 10^{11} \text{ cm}^{-2}$, based on solar abundance ratios for KI (Schempp *et al.* 1989)). For comparison, we also show the residual for the reference star HD12235 in Figure 6. This star was reduced in exactly the same manner as HD209458 and the stellar sodium D1 line was fit and removed using the same methods as for HD209458. As expected, no features were present in the spectra on either night. The 3σ upper limits are $1.1 \times 10^{10} \text{ cm}^{-2}$ (2002 August 28), and $9.4 \times 10^9 \text{ cm}^{-2}$ (2002 August 31), which are in agreement with our results for HD209458.

4.2. Detection Probability

Since no signal was detected we examine the likelihood of observing a comet crossing based on the amount of time the comet spends within an observable window. We only consider the orbit within 3 AU since comet features will not be significant beyond this distance from the star. The amount of time the comet spends in front of the star is determined by the diameter of the star, D_{sun} , and the tangential velocity, v_{tan} . This time will vary depending on the orientation of the orbit to our line of sight. The radius of HD209458 is $1.18R_\odot \approx 8.21 \times 10^5 \text{ km}$, which is comparable to the width of the sodium tail, $8 \times 10^5 \text{ km}$ (NASA Hale-Bopp website). For the total time in front of the star within a year for any comet in the system we multiply by the average number of periodic comets per year ~ 25 , ~ 10 of which are SP comets (Halley type) and ~ 15 of which are LP comets (Hale-Bopp type) (Krishna Swamy 1997). We double this since our observations are over the course of two years. The time that any SP comet spends in front of the star over two years ranges between 7 days and 35 days for v_{tan} varying from 11 km s^{-1} to 54 km s^{-1} , with an average time of in front of the star of 10 days. For LP comets the time ranges between 13 days and 42 days for v_{tan} varying from 14 km s^{-1} to 44 km s^{-1} , with an average time of 18 days in front of the star. Since our observing time is small compared to the time comets

spend in front of the star and observing a comet can be considered a random process, the probability can be efficiently described by a Poisson distribution $P(t, \tau) = 1 - e^{-\mu}$ where $e^{-\mu}$ is the probability of observing zero events over the total combined observing window, and $\mu = (\tau N)$ is the average number of events for the combined observations. τ is defined as the average number of comets observable at any time, which can be calculated by multiplying the total amount of time that a single comet would spend in the line of sight by the estimated number of comets per year and then dividing by the the total time (one year). N is the total number of chances to see a comet, defined as the total number of observing sessions. An observing session is defined as the period of time needed to reach a S/N necessary to detect sodium absorption. This calculation assumes that the observable windows for the different comets do not overlap, a reasonable assumption considering the estimated number of comets and amount of time each one spends in front of the star. Since the estimated number of comets per year can be considered to be constant over our monitoring period, the chances of observing a comet are insensitive to the elapsed time between observations, and depend only on the average number of comets per year in the system and the total number of observing sessions.

The probability as a function of the number of observing sessions for our long and short cometary models are plotted in Figure 7. The probability of detecting either type of periodic comet from 6 observations (in two years, 2001-2003), ranges from 16% to 55%, with an average probability of 20%. According to these probabilities then, we would need to make ~ 20 observations to achieve a 50% likelihood of observing a comet. As a more conservative estimate we only consider the scenario when we are looking directly into the sodium tail, which would maximize the column density. This then decreases D_{sun} to essentially the stellar radius and gives a probability of about half the values listed above and we would need to make double the amount of observations to be certain of a 50% chance. The probability could also vary depending on the number of comets in the system. In Figure 8 we show how the number of comets affects the probability using the average, minimum and maximum time a comet spends in front of the star and our current number of observations. There would need to be ~ 150 total comets per year for us to have a 50% chance with our current number of observations.

This implies that it would be necessary to either continue with more observations of this system or expand our target list to cover many more systems in order to have a better chance of detecting a comet event.

4.3. Theoretical Column Density

For comparison, we have also conducted theoretical calculations on the column density we would expect from typical comet events. Using measurements of comet Hale-Bopp we calculate an approximate column density of sodium in the tail. Using the production rate and lifetime of neutral sodium atoms listed in Cremonese *et al.* (1997) of $Q(\text{NaI}) \simeq 5 \times 10^{25}$ atoms s^{-1} and $\tau = 1.69 \times 10^5$ s at 1 AU (which for Hale-Bopp is very close to perihelion, $q=0.914$), we estimate the column density of the tail to be $4 \times 10^8 \text{ cm}^{-2}$. Soon after the discovery by Cremonese *et al.* (1997) of the sodium tail, Wilson *et al.* (1998) discovered that there was a second sodium tail (termed the diffuse sodium tail) superimposed on the dust tail with a production rate of sodium very similar to that determined for the pure sodium tail. If we consider the sodium in both sodium tails and the contribution of sodium in the coma, (which was estimated to be $Q(\text{NaI}) \simeq 1 \times 10^{25}$ atoms s^{-1} by Combi *et al.* (1997)), the total production rate increases to 1×10^{26} atoms s^{-1} and the column density to $\sim 8 \times 10^8 \text{ cm}^{-2}$. Combi *et al.* (1997) argue that, based on solar abundances and the production rate of oxygen (10^{30} cm^{-2}), the total production rate of sodium should be a few times 10^{27} cm^{-2} , which would lead to a column density of $\sim 8 \times 10^9 \text{ cm}^{-2}$. Based on our upper limits we would be able to detect a feature of this column density if it were offset from the rest wavelength of the star. This is likely since from Figure 2 it is shown that the majority of the orbit will produce at least a 0.4 \AA shift. The upper limits determined in the previous section are on the order of the column density of sodium from a single periodic comet, which verifies that we would be able to detect the passage of a single comet. With the probability, this suggests an upper limit of ~ 300 total comets per year that come within 3 AU of HD209458 (based on a 95% probability(2σ)). Considering that the β Pictoris system has ~ 300 -1000 FEB's per year (Lagrange *et al.* 1992; Ferlet *et al.* 1993), this upper limit is consistent with a more evolved system.

5. Conclusion

We monitored the planet-bearing solar-type star HD209458 for comet activity using the HET over the course of 2 years with 6 observations with S/N ratios between 70 and 258. Our observations of the sodium D1 line were examined for variable absorption components, as seen in β Pictoris and other stars, which are considered to be signatures of this type of activity. From modelling, we determined that a feature with a detectable column density of $\sim 10^{10} \text{ cm}^{-2}$ would have a FWHM of $\sim 0.05 \text{ \AA}$ and a W_λ of $\sim 1 \text{ m\AA}$ and could be shifted up to $\sim 0.5 \text{ \AA}$ from the photospheric line center. Simulations based on typical solar system periodic comets showed that the probability of a detection from 6 observations was $\sim 20\%$

and was insensitive to the total elapsed time between observations. The probabilities derived suggest that less than ~ 300 total comets per year come within 3 AU of HD209458 or one would have likely been detected. No absorption features greater than 3σ due to cometary activity were identified. Our upper limits for the sodium column density for each observation are consistent with the column density expected from the sodium tail of solar-type comets. Some possible reasons for the non-detection are

1. The small number of observations. This system is expected to have comet activity on a similar scale as the solar system since it is a ~ 5 Gyr old solar-type star (Cody & Sasselov 2002). With only 6 observations in 2 years, our chances of witnessing a comet crossing were quite small. We plan to continue to monitor this star with many more observations.
2. A comet was passing but it was not detectable to us. The inclination of the comets orbit might have been such that it was not within our line of sight. Though, in the solar system, 87% of short period comets have inclinations within 30° and 81% have perihelia latitudes less than 10° from the ecliptic (all of them are within 30°) (Biswas 2000). Long period comet inclinations are more scattered about the ecliptic, with only 47% having inclinations less than 90° and 63% having perihelia latitudes less than 30° (Biswas 2000). So, inclination may factor into the probability when considering long period comets.
3. The sodium feature was at the rest wavelength of the star. This would occur if the comet was detected at perihelion, which would be a less likely circumstance for periodic comets since they spend only a small fraction of their time there. If it were the case though, based on estimates of the column density of the sodium tail from a single comet, our S/N in the core of the D1 line might not be sufficient to uncover a signal. For our future observations we plan to obtain higher S/N data.

Continued monitoring of HD209458 will occur over the next year, and observations are planned for several other planet-bearing stars. Through continued observations we can improve our upper limits for the number of comets in the planetary system around HD209458 and increase our chances of detecting a cometary event.

We would like to thank John Debes for helping to initiate the observations and for the use of his absorption profile code. We also thank Robin Ciardullo for his helpful discussions concerning probability. This work was supported by NASA grants NGA5-12115, NAG5-11427, and NAG5-13320, NSF grants AST-0138235 and AST-0243090 and the Penn State Eberly College of Science.

REFERENCES

- Beust, H. and Morbidelli, A. 2000, *Icarus*, 143, 170-188
- Beust, H., Lagrange, A.M., Crawford, I.A., Goudard, C., Spyromilio, J., & Vidal-Madjar, A. 1998, *A&A*, 338, 1015-1030
- Biswas, S.N. 2000, *Bull. Astr. Soc. India*, 28, 539-578
- Charbonneau, D., Brown, T.M., Noyes, R.W., & Gilliland, R.L. 2002, *ApJ*, 568, 377-384
- Charbonneau, D., Brown, T.M., Latham, D.W., & Mayor, M. 2000, *ApJ*, 529, L45-L48
- Combi, M.R., DiSanti, M.A., & Fink, U. 1997, *Icarus*, 130, 336-354
- Cody, A.M. & Sasselov, D.D. 2002, *ApJ*, 569, 451-458
- Cremonese, G. 1997, *Space. Sci. Reviews*, 90, 83-89
- Cremonese, G., Boehnhardt, H., Crovisier, J., Rauer, H., Fitzsimmons, A., Fulle, M., Licandro, J., Pollacco, D., Tozzi, G.P., & West, R.M. 1997, *ApJ*, 490, L199-L202
- Ferlet, R., Lagrange-Henri, A.M., Beust, H., Vitry, R., Zimmermann, V.P., Martin, M., Char, S., Belmahdi, M., Clavier, J.P., Coupiac, P., Foing, B.H., Sevre, F., & Vidal-Madjar, A. 1993, *A&A*, 267, 137-144
- Ferlet, R., Hobbs, L.M., & A. Vidal-Madjar 1987, *A&A*, 185, 267-270
- Ge, J. 1998, Ph.D Dissertation, The University of Arizona
- Grady, C.A., Sitko, M.L., Bjorkman, K.S., Perez, M.R., Lynch, D.K., Russell, R.W., & Hanner, M.S. 1997, *ApJ*, 483, 449
- Grinin, V.P., Kozlova, O.V., The, P.S., & Rostopchina, A.N. 1996, *A&A*, 309, 474-480
- Hobbs, L.M., Albert, C.E., & Gry, C. 1985, *ApJ*, 293, L29-L33
- Ibukiyama, A. & Arimoto, N. 2002, *A&A*, 394, 927-941
- Iseli, M., Kuppers, M., Benz, W., & Bochsler, P. 2002, *Icarus*, 155, 350-364
- Jewitt, D. & Matthews, H. 1999, *ApJ*, 117, 1056-1062
- Krishna Swamy, K.S. 1997, *Physics of Comets* 2nd Ed.

- Lagrange-Henri, A.M., Gosset, E., Beust, H, Ferlet, R., & Vidal-Madjar, A. 1992, *A&A*, 264, 637-653
- Lagrange-Henri, A.M., Vidal-Madjar, A., & Ferlet, R. 1988, *A&A*, 190, 275-282
- Lagrange, A.M., Ferlet, R., & Vidal-Madjar, A. 1986, *ESA Proc. Eight years of UV Astro. with IUE*, 569-571
- Morton, D.C. 1991, *ApJ Suppl. Series*, 77, 119-202
- NASA Goddard Space Flight Center, Hale-Bopp website,
<http://www.gsfc.nasa.gov/ftp/pub/pao/releases/1997/97-40.htm>
- Oppenheimer, M. 1980, *ApJ*, 240, 923-928
- Schempp, W.V. & Hayden Smith, W.M. 1989, *PASP*, 101, 431-433
- SOHO sungrazer website, <http://sungrazer.nascom.nasa.gov/>
- Sorelli, C., Grinin, V.P., & Natta, A. 1996, *A&A*, 309, 155-162
- Stern, Alan S. 1993, Southwest Research Institution, Instrumentation and Space Res. Div., Semiannual Report No. 2
- Tull, R.G. 1998, *SPIE*, 3355, 387-398
- Vidal-Madjar, A., Lecavelier des Etangs, A., Desert, J.M., Ballester, G.E., Ferlet, R., Hebrard, G., & Mayor, M. 2003, *Letters to Nature*, 422, 143-146
- Watanabe, J., Kawakita, H., Furusho, R., & Fujii, M. 2003, *ApJ*, 585, L159-L162
- Welsh, B.Y., Craig, N., Crawford, I.A., & Price, R.J. 1998, *A&A*, 338, 674-682
- Wilson, J.K., Mendillo, M., & Baumgardner, J. 1998, *Geophys. Res. Letter*, 25, 225
- Zeilik, M. & Gregory, S.A. 1998, *Intro. Astro. & Astroph.* 4th ed.

line =

Table 1. Observations

Star	Observation Date	Heliocentric Velocity km/s	Number of Exposures	Time per Exposure seconds
HD209458	2001 Jul07	21.29	4	500
	2001 Jul09	20.78	2	900
	2002 Oct10	-16.4	2	1500
	2002 Nov23	-26.36	2	1500
	2002 Dec09	-26.46	2	1500
	2003 Jul14	19.60	1	3600
HD12235	28Aug02	23.60	2	1200
	31Aug02	22.70	3	1000

Table 2. Stellar Parameters

Object	Age Gyr	Spectral Type ^a	Radius ^b R_{\odot}	Teff ^b K	L ^b L_{\odot}	Vmag ^a	Radial Velocity ^a km/s
HD209458	5.2 ^b	GOV	1.18	6000	1.61	7.7	-14.8
HD12235	5.39 ^c	G2IV				5.9	-17.4

^aReference-SIMBAD data retrieval system (of the Astronomical Data center in Strasbourg, France)

^bReference-Cody & Sasselov (2002)

^cReference-Ibukiyama & Arimoto (2002)

Table 3. Sodium Column Density Upper Limits of HD209458 System.

Observation Date	S/N in continuum	N(NaI) Upper Limit cm^{-2}	S/N in line core	N(NaI) Upper Limit cm^{-2}
7July01	70	2.2×10^{10}	23	6.5×10^{10}
9July01	110	1.4×10^{10}	36	4.3×10^{10}
10Oct02	198	7.6×10^9	67	2.3×10^{10}
23Nov02	237	6.4×10^9	88	1.7×10^{10}
9Dec02	258	5.8×10^9	88	1.7×10^{10}
14July03	204	7.4×10^9	67	2.2×10^{10}

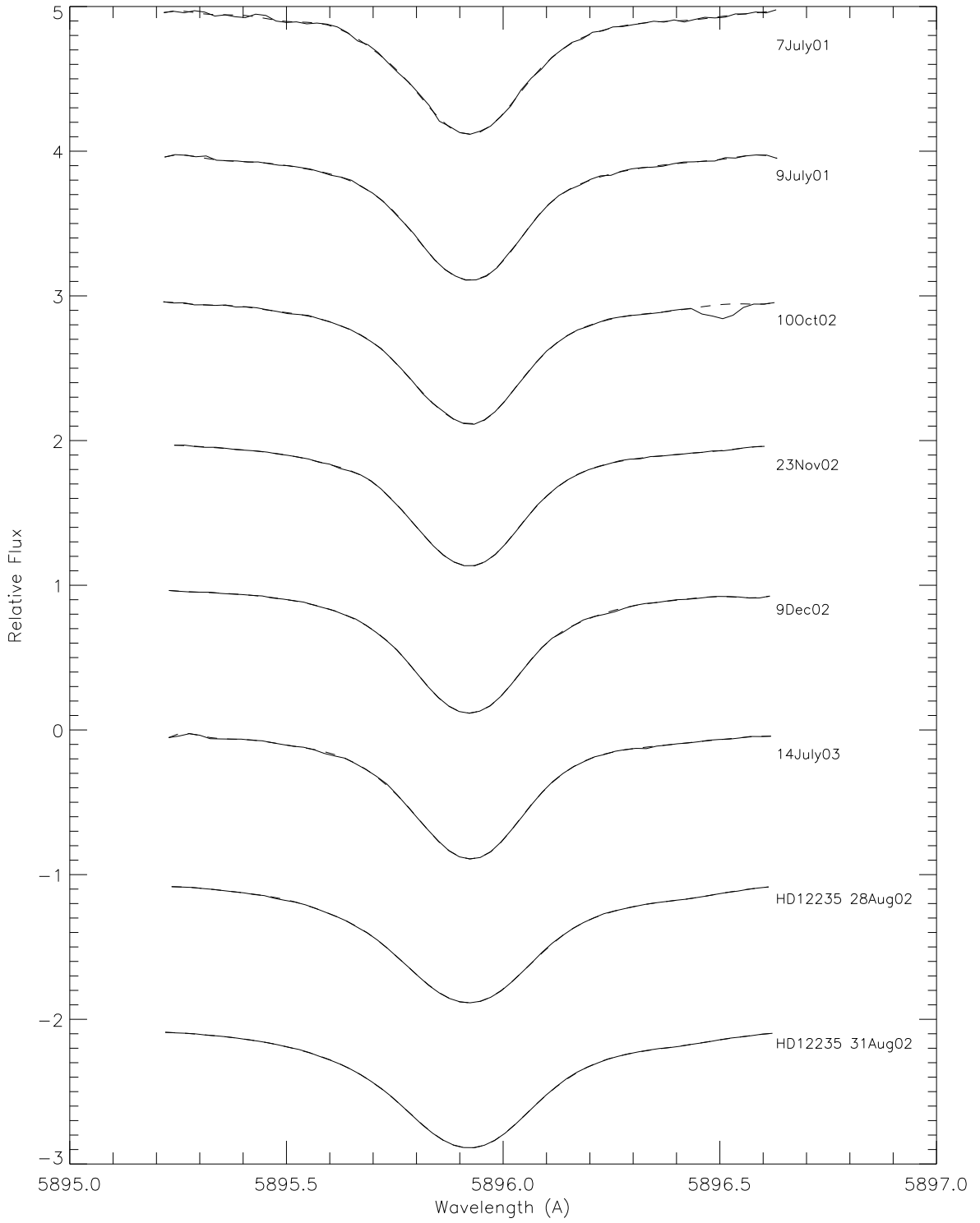


Fig. 1.— HD209458 on all 6 nights and HD12235. The fit to the D1 line is overplotted with a dashed line. The spectra have been shifted to the rest frame of the system.

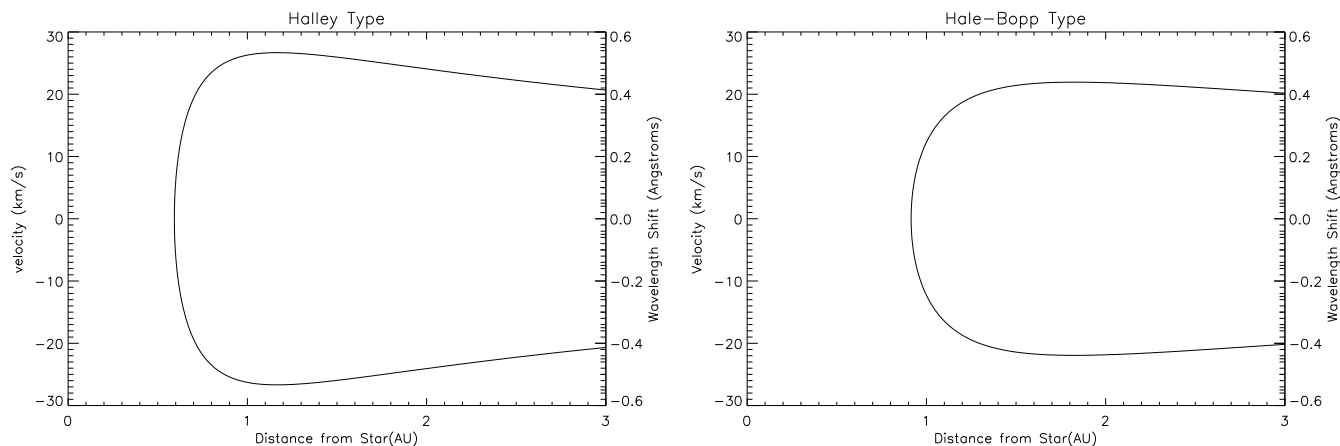


Fig. 2.— Wavelength and corresponding doppler shift due to the tail velocity for (Left) Short period comets and (Right) Long period comets. The above plots show that the greatest wavelength shift expected would be 0.53 \AA from the photospheric line center.

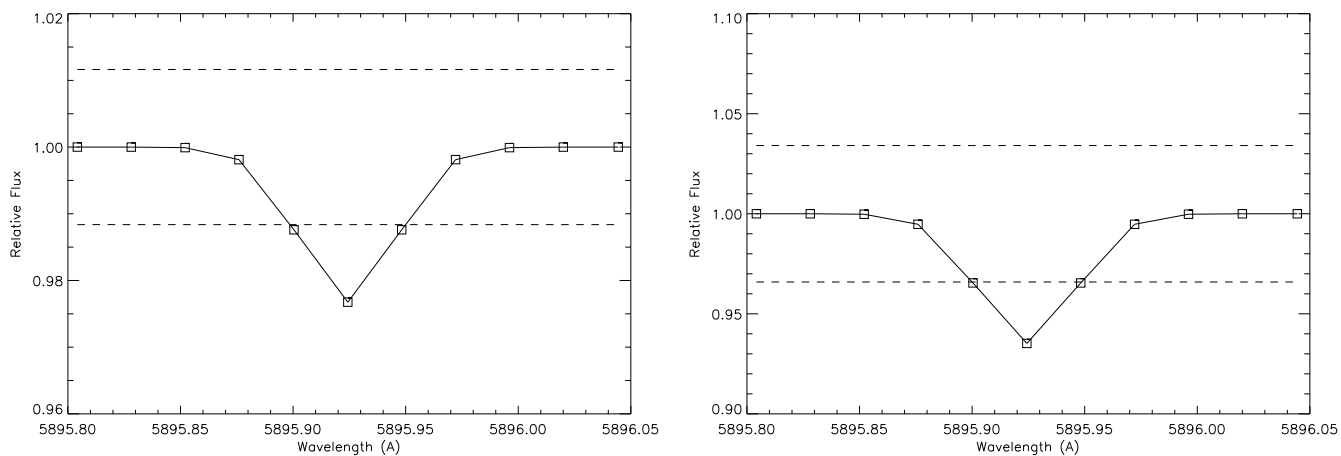


Fig. 3.— Theoretical Sodium Absorption Line. (Left) Column density of $5.8 \times 10^9 \text{ cm}^{-2}$ based on upper limit of best S/N in the continuum (~ 260 for 2002 Dec 09). Dashed lines represent 3σ . (Right) Column density of $1.7 \times 10^{10} \text{ cm}^{-2}$ based on upper limit of best S/N in the core of the D1 line (~ 90 for 2002 Dec 09). Dashed lines represent 3σ .

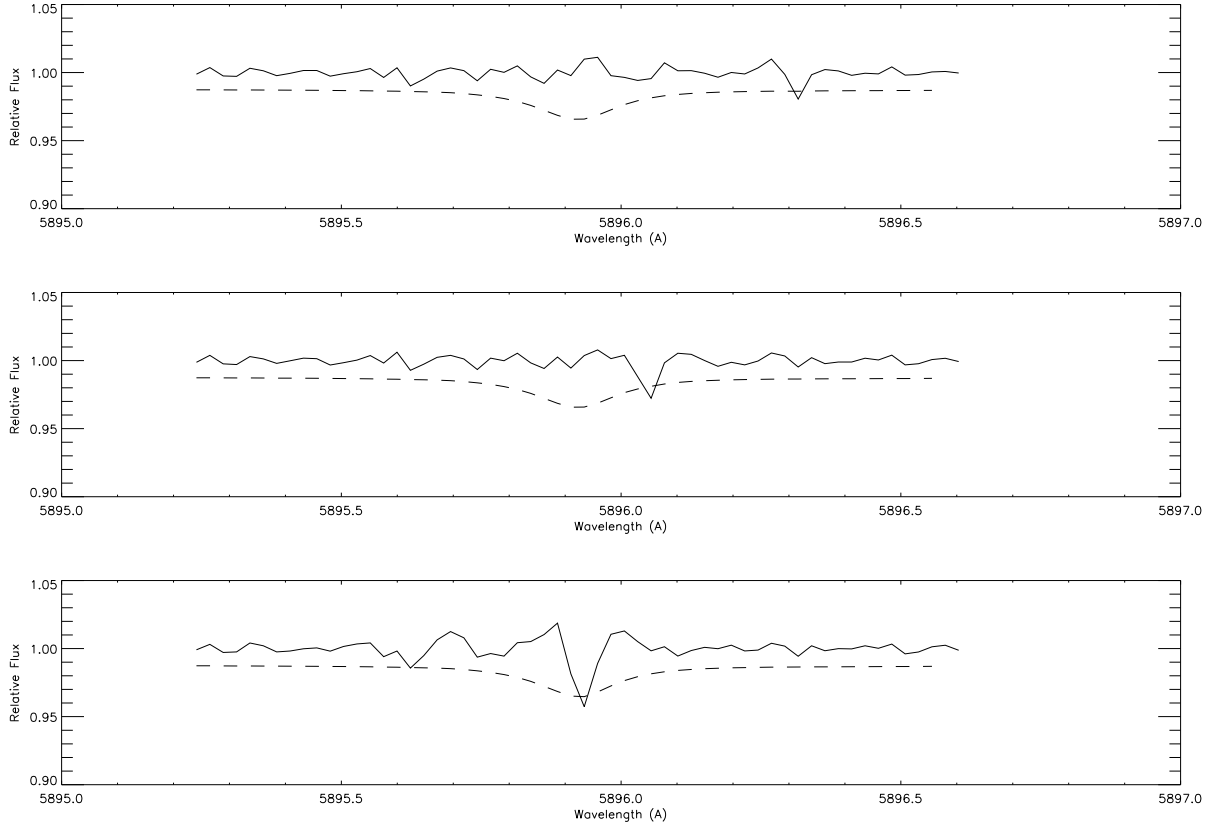


Fig. 4.— Residual from polynomial fit to the 2002 November 23 stellar sodium D1 profile. The absorption feature is a sodium synthetic feature in the continuum region with $N(\text{NaI})=6.4 \times 10^9 \text{ cm}^{-2}$ (Top) in the wing with $N(\text{NaI})=9.3 \times 10^9 \text{ cm}^{-2}$ (Middle) and in the core with $N(\text{NaI})=1.7 \times 10^{10} \text{ cm}^{-2}$ (Bottom). Column densities from 3σ upper limits listed in Table 3. Dashed lines represent 3σ .

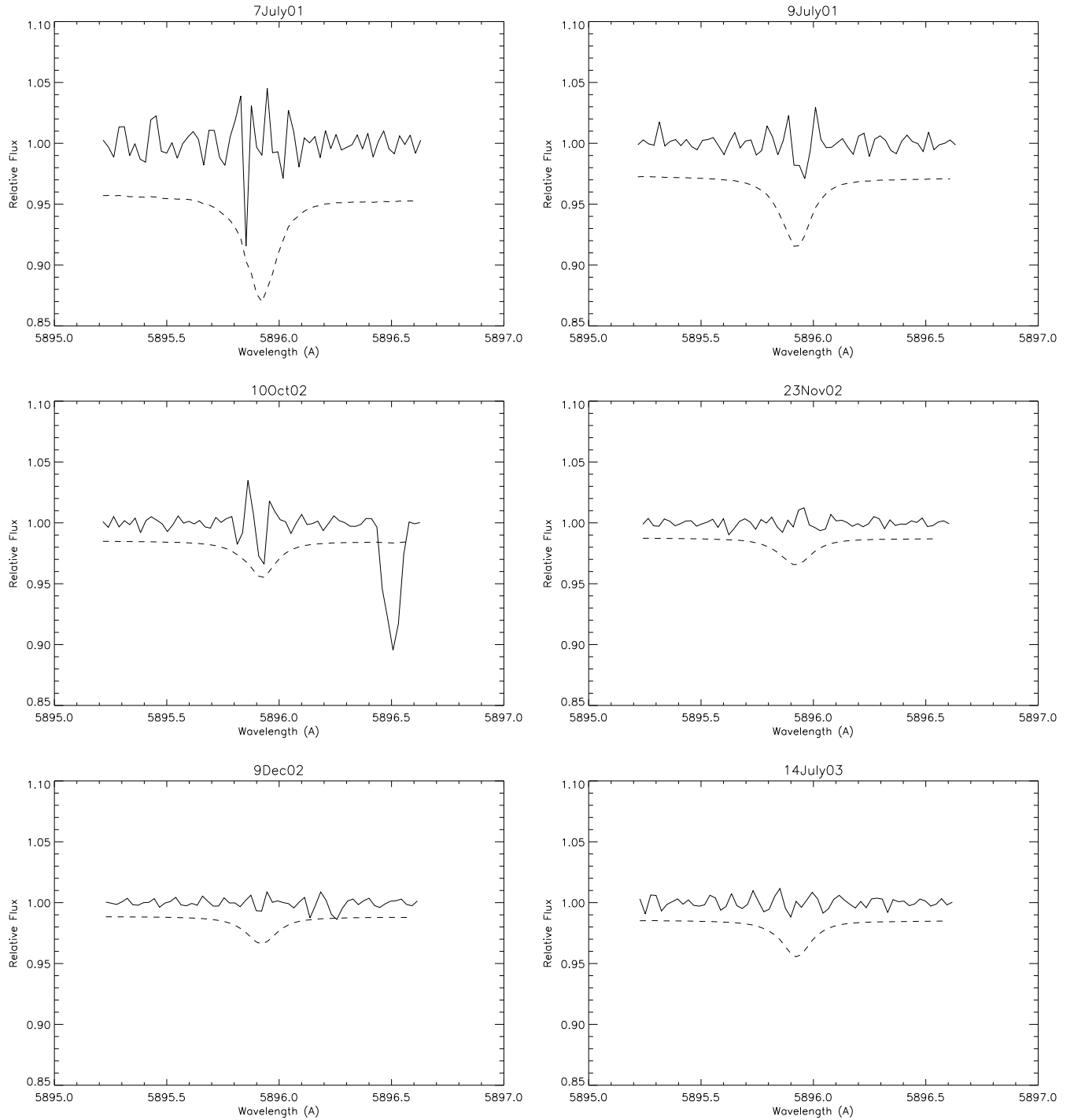


Fig. 5.— Residual from polynomial fit to the photospheric D1 profile. Dashed line represents 3σ . In 2002 October 10 the absorption feature at 5896.5 Å is from a telluric line that was poorly removed.

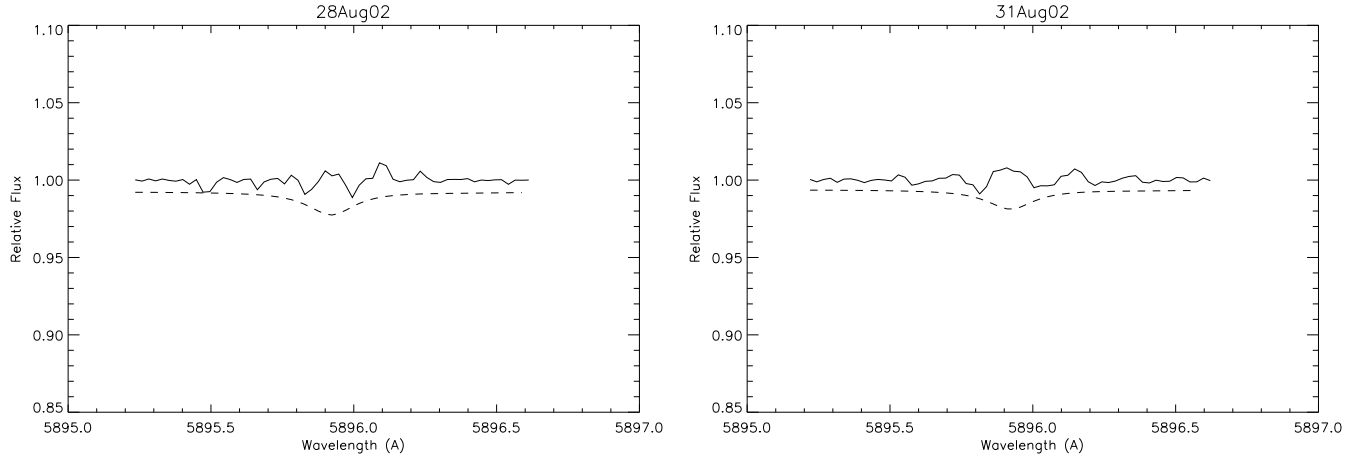


Fig. 6.— Reference star HD12235. Residual from polynomial fit to the photospheric D1 line. Dashed line represents 3σ .

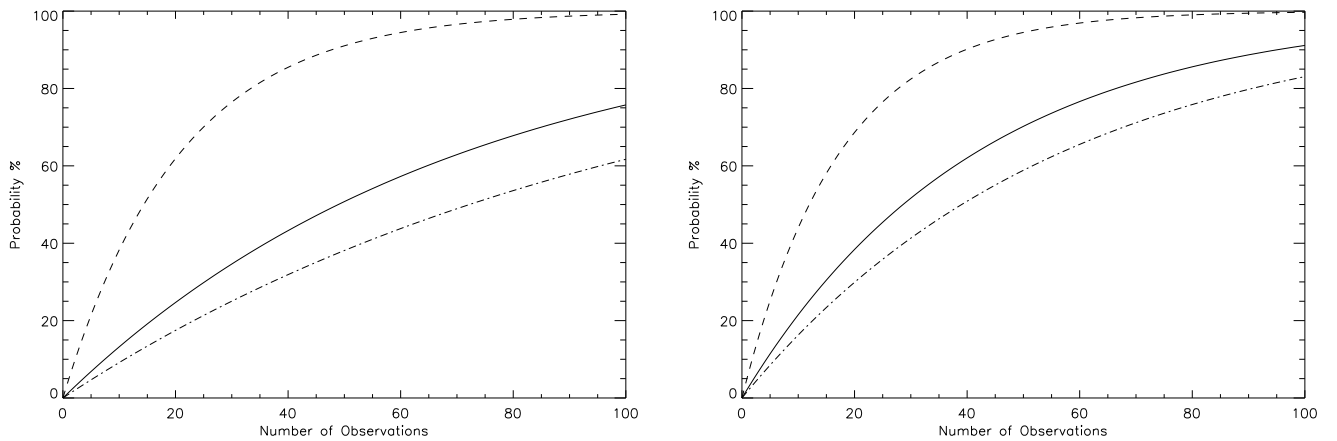


Fig. 7.— Probability of detection based on number of observations and total number of comets per year=10 SP and 15 LP. Dashed line=maximum probability, solid line=average and dotted/dashed line=minimum. (Left) Short period comets (Right) Long period comets.

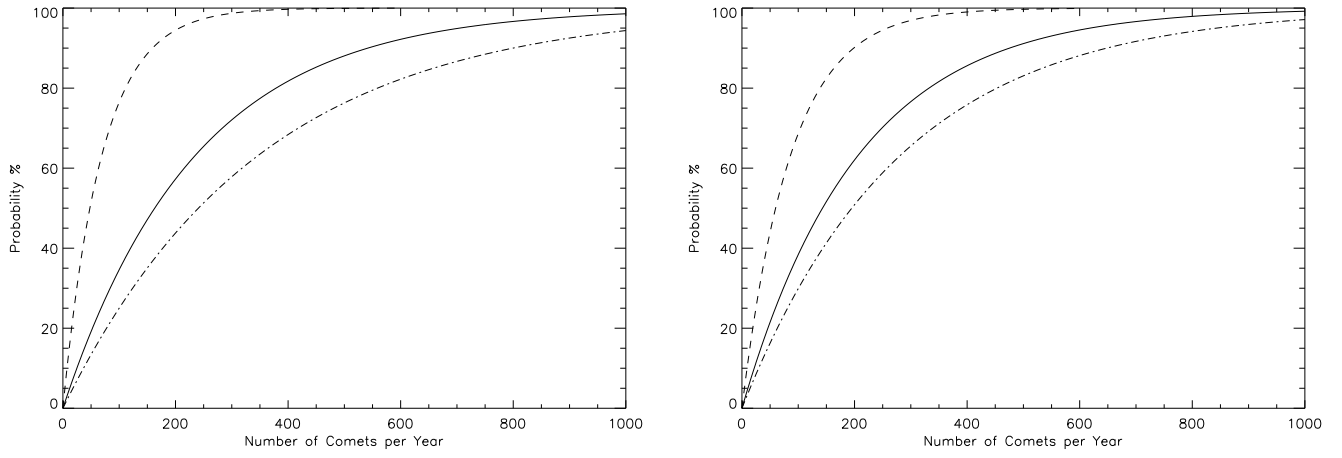


Fig. 8.— Probability of detection based on number of comets per year and our total number of observations=6. Dashed line=maximum probability, solid line=average and dotted/dashed line=minimum. (Left) Short period comets. (Right) Long period comets.